

Electrical analysis of hysteresis in solution processed silicon nanowire field effect transistors

K. Prabha Rajeev, C. Opoku, V. Stolojan, M. Constantinou and M. Shkunov*

Electronic Engineering, Advanced Technology Institute, University of Surrey, Guildford GU2 7XH, UK

Abstract Silicon nanowires (Si NW) are ideal candidates for solution processable field effect transistors (FETs). The interface between the nanowire channel and the gate dielectric plays a crucial role in the FET performance, and it can be responsible for unwanted effects such as hysteresis of the I-V characteristics due to threshold voltage shift when the gate voltage is applied. Using gate-voltage bias stress measurements we show that a large hysteresis of up to 40V in Si NW FETs with SiO₂ dielectric is mainly due to the holes traps at the nanowire/SiO₂ interface. An approach for reducing this hysteresis to just 2.5V using solution processable fluoropolymer dielectric Cytop in the top-gate configuration is demonstrated. Experimental results suggest that the density of surface traps in Si nanowire transistors is dictated mainly by the nature of the dielectric layer. The influence of the gate dielectric was studied by assessing the field effect transport behaviour of a representative double gate FETs based on SiO₂ bottom dielectric and top a Cytop dielectric layer. Such devices were characterised, revealing an order of magnitude higher hole traps density at the nanowire/SiO₂ interface ($1 \times 10^{13} \text{cm}^{-2}$) compared to that of nanowire/fluoropolymer interface ($7.5 \times 10^{11} \text{cm}^{-2}$).

Key words hysteresis, silicon nanowires, field effect transistor, polymer dielectric, surface states

* email: m.shkunov@surrey.ac.uk

1. Introduction

Solution-processed printable electronics using semiconducting inks have opened up the possibility of various low-cost electronic devices targeting large area applications such as RFID tags[1], sensor[2], displays[3] where semiconductor is deposited via various printing methods compatible with a wide range of substrates including plastics. Currently, the materials of choice for large area electronics are amorphous silicon (a-Si), polycrystalline silicon (poly-Si) and organic semiconductors. However, the high temperatures required for processing of amorphous silicon or polysilicon transistors make it very challenging to use them on low-cost plastic substrates[4]. Conversely, organic semiconductors can be deposited at low temperatures, but their charge carrier mobility in printable FETs is limited to few cm^2/Vs [5]. Nanomaterials such as inorganic semiconducting nanowires offer very high mobilities[6], and their low temperature processing[7] makes them ideal candidates for printable electronics. Growth methods such as chemical vapour deposition growth[8], vapour-liquid-solid growth[9] can produce high quality nanowires, with lengths compatible with typical transistor channel dimensions. However, such synthesis methods are limited to small substrate size thus making them impractical for industrial scale processes. Korgel's group[10] has demonstrated that the supercritical fluid liquid solid (SFLS) method for growing Si nanowires can be industrially scalable, with a throughput of few kilograms per day is achievable. The ability to disperse these nanowires in different solvents to make ink formulation shows their potential for printing deposition technologies. The separation of the synthesis process from the devices assembly enables the fabrication of electronics at low processing temperatures.

In order to fully realise the potential of solution processable Si NWs in the area of high performance transistors, some of the key issues need to be addressed such as: i) alignment of Si nanowires to form 'monolayer' of ordered arrays to bridge the source-drain electrodes, and ii) elimination of surface states to reduce I-V characteristics hysteresis and increase the device mobility.

Various alignment deposition techniques, such as directed flow assembly[7], DNA hybridisation assembly[11], electrostatic force assembly[12], Langmuir- Blodgett technique[13, 14], dielectrophoresis alignment[15, 16] have been demonstrated, however, the majority of these techniques cannot be applied to large area deposition or they involve laborious fabrication steps to do so[7]. A high quality alignment, where nanowires do not cross each other is essential to avoid gate screening effect for high performance FETs. Thus, a low-cost and large substrate area compatible nanowires alignment techniques are still required.

Nanowires possess high surface area, and charge transport is strongly affected by the quality of semiconductor surface. In particular, the device mobility and hysteresis in Si NW FETs are influenced by the nanowire/gate-dielectric interface, due to the trapping of charge carriers. Commonly used gate dielectric for Si NW FET fabrication is thermally grown silica (SiO₂). SiO₂ dielectric is known to contain surface bound hydroxyl (OH⁻) groups[17, 18]. These groups induce interface states that can trap accumulated charges during FET characteristics. The trapping is typically manifested as hysteresis behavior during transistor I-V scans. Hysteresis is the shift in threshold voltage (ΔV_{th}) during the forward (+V to -V) and the reverse gate voltage sweep (-V to +V) at constant drain voltage bias. The mobility in a-Si FETs using *high-k* gate dielectrics is compromised due to scattering mechanism from fixed charges[19], and an increase in hysteresis is reported for Si NW FETs due to the surface adsorbed OH⁻ groups[18]. Elimination of hysteresis in a device will improve the overall FET performance including the device field effect mobility, due to less scattering of charge carriers. Passivation of devices with poly (methyl methacrylate) on PbSe nanowires or self-assembled monolayers on Si NWs has shown to remove the surface bound hydroxyl group, thereby reducing the hysteresis. It has also been reported that SiO₂ thermally grown at high temperatures (~1100°C) on Si NW reduces the hysteresis in the corresponding nanowire FETs, but such high temperature treatment is not compatible with flexible substrates [20, 21]. Gate dielectrics which have low affinity towards OH⁻ groups such as silicon nitride (*a*-SiN_x) have shown increased mobility in *a*-Si thin film transistors due to less interface charging[22], but the high temperature required for the deposition of the *a*-SiN_x (~ 250°C - 450°C) makes them incompatible with plastic substrates. However, low *k* insulators such as organic dielectrics, have surfaces with low energetic disorder which were investigated in organic field effect transistors[23]. Reduced hysteresis and enhanced mobility can be achieved by using hydrophobic polymers as gate dielectrics instead of SiO₂, with low amount of OH⁻ trap sites at the nanowire/dielectric interface[24].

In this work, we have deposited SFLS grown Si NWs via a roll-cast technique to give ordered arrays of nanowires and to remove nanowire aggregates and impurities clusters from the nanowire layers. Gold electrodes were used as source/drain contacts in the Si NW FETs to provide near-ohmic contacts. The nature of traps causing hysteresis was studied using sweep rate study and bias stress measurement of transistors with SiO₂ as dielectric, in bottom-gated geometry. The effect on hysteresis using a fluoropolymer (Cytop with $\epsilon_r \sim 2.1$) as the gate dielectric was studied in top gate device geometry. Finally a comparison of SiO₂ and fluoropolymer as gate dielectrics in a dual-gate configuration of the same FET device was conducted showing significant reduction of surface trap density at nanowire/polymer interface compared to nanowire/silicon oxide interface.

2. Experimental details

Silicon nanowires used in this work were synthesised by the supercritical-fluid liquid solid method, as described elsewhere[10]. The formulations of Si NWs dispersed in anisole were used to prepare samples for SEM and TEM analysis by drop casting a small amount of dispersion on Si/SiO₂ substrates and on a holey-carbon grid (Agar Scientific), respectively. SEM images of as-grown Si nanowires were used to evaluate the NW lengths to be from 2µm to 100µm. Most of nanowires were within 5-30µm length range. Figure 1(a) shows TEM image of a network of Si nanowires with a noticeable amount of impurities, nanowire aggregates and defective kinked nanowires. High resolution TEM in Figure 1(b) show a typical straight single nanowire with a diameter of ~ 35nm surrounded by a 4nm thick amorphous polyphenylsilane shell. The nanowire growth direction was identified from computed Fast Fourier Transform (FFT) pattern obtained from the lattice fringes (Fig. 1(b)) to be along [110], which is consistent with previous reports[10].

Nanowires were deposited on the substrates using a roll-cast coating method. The nanowire formulation was drop-casted on the part of the inclined substrate, and a glass roller was placed at the top of the substrate and then allowed to roll down under the influence of the gravitational force. The roller was making contact with the substrate, enabling to spread out the nanowire formulation and to remove protruding clumps, stacked nanowires and large impurity particles. Additionally, the shear force induced by the roller movement was acting on nanowires to produces preferential alignment along the rolling direction (supporting information, Figure S1). The nanowires density on the substrate can be increased by repeating the process, until the required density is achieved. The nanowire alignment can be improved by using a compressed air gun to dry the solvent immediately after the roll-casting process. Following the nanowire deposition the substrates were dried and prepared for photolithography.

The source-drain transistor electrodes were patterned using photolithography (lift-off) on top of the aligned nanowires by sputtering Cr/Au (3nm/50nm) contacts. Bottom-gate FETs were fabricated on Si/SiO₂ substrates,

whereas top-gated FETs were prepared on low sodium glass substrates. Following the contacts deposition the substrates were annealed at 200°C in N₂ filled glove box, to improve charge injection/extraction at the nanowire-contact interface. For top-gate transistor devices fluoropolymer Cytop was spin coated on top of deposited nanowires with source-drained patterned electrodes; and then baked (100°C, 10min) in air. A 50nm thick Au gate electrode was evaporated through a shadow mask on top of the channel area covered with gate dielectric. The double gate devices were fabricated by preparing a bottom gate FET on Si/SiO₂ substrate and then completing the structure with a top gate insulator (Cytop) and a gate electrode.

Transistor characterisation and the gate-voltage bias stress measurements were performed with Agilent 4155C semiconductor analyzer in N₂ filled glove box to minimize the environmental effect which can cause traps due to surface bound OH⁻ groups and adsorption of polar water molecules onto the nanowire or nanowire/dielectric interfaces.

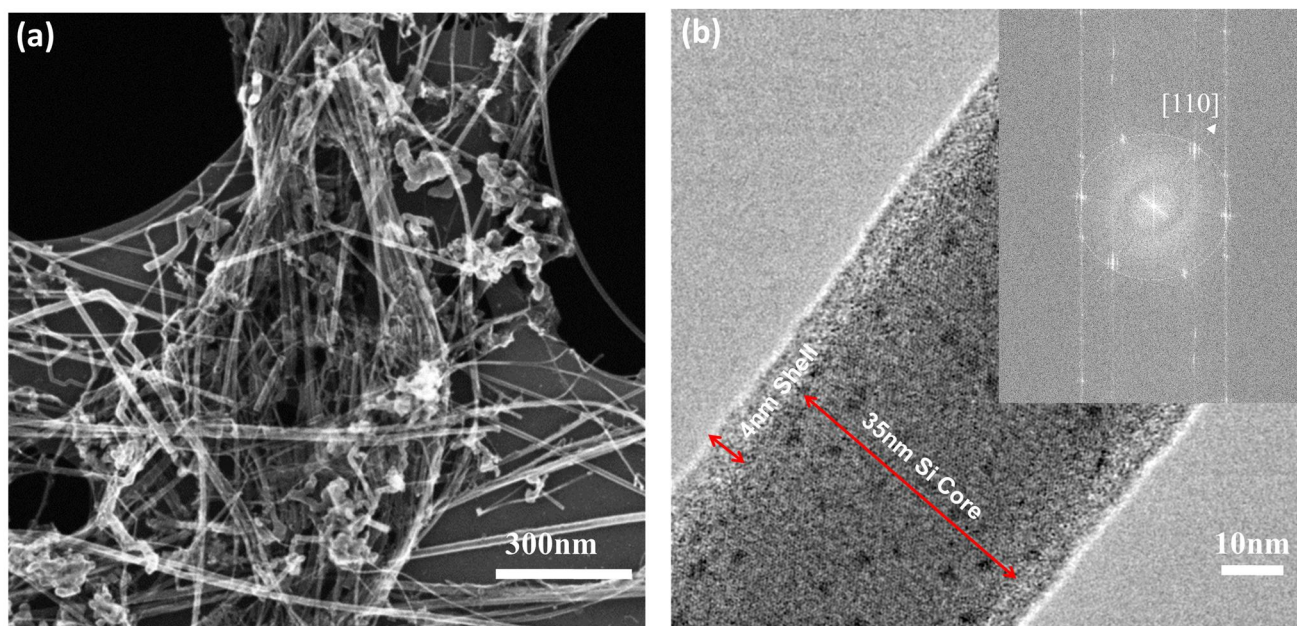


Figure 1. Characterisation of SFLS-grown silicon nanowires. (a) TEM secondary electron image of a network of nanowires showing impurity particles and clumps of nanowires. TEM carbon grid is visible on the background, (b) High resolution TEM (HRTEM) image of a single nanowire with 35nm core diameter and 4nm thick amorphous shell. The inset illustrates FFT of the nanowire showing the growth direction [110].

3. Results and discussion

3.1 Bottom gate vs top gate Si - NW FETs

Figure 2(a) shows the transfer characteristics of the Si-NW FETs (23 nanowires in the channel) with SiO₂ as gate dielectric, with channel length of 5µm. The drain current (I_D) was obtained by scanning the gate voltage from +20V to -60V in the forward voltage sweep and from -60V to +20V in the reverse voltage sweep, at a -5V and -10V drain bias voltages (V_D). The gate voltage sweep rate was kept constant at 1 V/s throughout the measurement. A lower gate voltage sweep rate is chosen to study the extent of trapping and trap depletion at the Si NW/SiO₂ interface. In our studies, we have observed that the hysteresis increases with decreasing gate sweep rate, indicating the presence of slow filling traps. From the transfer characteristics in Figure 2 (a), a p-type behavior is observed showing charge accumulation at negative bias gate voltages. The device shows an excellent gate modulation for a common back-gated transistor with an I_{ON}/I_{OFF} ratio of 10^6 , and a turn ON voltage at -2V. An increase in I_{ON} with V_D indicates good gate to channel coupling. The hysteresis (ΔV_{th}) was extracted by taking the difference of threshold voltages obtained from forward gate sweep current (I_D) and reverse sweep (Supporting Information (SI) Fig.S2). A large hysteresis of $\sim 30V$ was observed at -5V drain voltage whereas the hysteresis decreased to $\sim 24V$ at -10V drain bias (Fig.2(a)). The decrease in hysteresis at high V_D can be attributed to the faster de-trappings of charge carriers at higher lateral electric field. A subthreshold swing (SS

= $\Delta V_G / \Delta \log I_D$) of 1.8V/decade and transconductance ($G_m = \partial I_D / \partial V_G$) of 0.6 μ S were estimated from the transfer characteristics.

The transfer characteristics of the top-gated Si-NW FETs with fluoropolymer dielectric are shown in Figure 2 (b). The device has a channel length of 2.5 μ m with 4 nanowires bridging the source-drain electrodes. The hysteresis is reduced significantly more than an order of magnitude, when compared to bottom gate Si NW device with SiO₂ dielectric. The measured hysteresis is \sim 2.3V at -5V drain bias, which indicates less trapping of charge carriers at the Si NW/polymer dielectric interface. There is no significant change in hysteresis when measured at a higher drain bias voltage (V_D -10V). High I_{ON}/I_{OFF} ratio of $> 10^7$ is obtained with transconductance of 0.6 μ S. The subthreshold swing (SS) was estimated to be \sim 3.3V/decade. The higher SS for top gate Si-NW FETs is due to the larger thickness of Cytop (1 μ m) compared to 230nm thick SiO₂ for bottom-gated devices, and also lower dielectric constant.

To extract charge carrier mobility the parasitic capacitance and fringing of the gate field due to the cylindrical nature of the nanowires should be taken into consideration. The nanowire FET mobility was estimated in the linear regime using the following equations [25-27]:

$$\mu = G_m \times \frac{L^2}{V_D C_n} \quad (1)$$

$$C_n = N \times \frac{2\pi\epsilon_o\epsilon_{ins}L}{\cosh^{-1}\left(\frac{r+d}{r}\right)} \quad (2)$$

Where C_n is the capacitance based on cylinder on a plate model for N number of nanowires in the FET channel with radius r and gate dielectric thickness d . L is the channel length, ϵ_o is the absolute permittivity, ϵ_{ins} is the gate insulator dielectric constant and V_D is the drain bias voltage. A capacitance of $\sim 7.2 \times 10^{-15}$ F was calculated for Si-NW FETs on SiO₂ using equation (2), whereas capacitance of Si-NW/Cytop structure was $\sim 2.5 \times 10^{-16}$ F. Using equation (1), we have calculated that the Si-NW FET mobility increased from 8 cm²/Vs for the bottom gate device to 14 cm²/Vs for top-gate device with Cytop dielectric. The increase in mobility for Si-NW/Cytop FETs is due to the less traps present at the interface, reducing the scattering of charge carriers. The change in hysteresis was compared for SiO₂ and organic polymer dielectric measured for several devices and they all showed similar pattern. (See Supporting Information, Figure S2). The hysteresis values for SiO₂ dielectric FETs were up to 40V, and typical ΔV_{th} values were in the range of 15V to 40V (SI Fig.S3). Devices with Cytop dielectric had significantly lower hysteresis, below 10V, with 50% of devices showing ΔV_{th} of less than 3V. The nature of traps in the SFLS-grown Si-NW FETs was analysed using gate-voltage bias stress measurement, as discussed in the next section.

3.2 Gate voltage bias stress measurement

Gate voltage bias stress experiments was carried out to determine if the observed hysteresis in Si-NW FETs is due to majority carrier (holes) trapping or minority carrier (electrons) trapping at the Si-NW/dielectric interface. The transfer characteristics of Si-NW/SiO₂ and Si-NW/Cytop FETs were initially measured before the gate voltage bias stress measurements. Then the gate electrode was biased at a constant -40V voltage for 30mins, and transfer characteristics were immediately measured, at a drain bias of -10V. The stress cycles were repeated for a total of 12hrs, with 30min stress time periods followed by transfer characteristics measurements. The stress measurements with +40V gate bias voltage was performed after the negative voltage bias stress, with the same stress measurement cycles for 12hrs. Figure 2(c) shows the extracted hysteresis values from the transfer characteristics of Si-NW/SiO₂ FET, for the gate bias stress measurements. It is observed that the hysteresis decreased to \sim 19.3V after the -40V gate bias compared to an initial value of \sim 29.1V, whereas the hysteresis increased from 24.4V to \sim 31.4V after +40V gate voltage stress. The threshold voltage also shifts to a further negative values (\sim -12V) after the -40V stress voltage compared to the initial threshold voltage of \sim -16V, however, the threshold voltage after +40V bias stress has decreased to \sim -2V (see SI, Figure S4). A lower hysteresis is observed after the negative gate-voltage stress due to the trapping of holes, thereby filling the long-lived traps with charge carriers. This experiment indicates that most of the traps will be occupied with holes during the 30min hold time of -40V gate-voltage stress, resulting in a higher reverse I_D and lower hysteresis. Whereas during positive gate-voltage bias stress, holes get de-trapped. This effect results in density increase of unoccupied traps present during the following I-V measurements, thereby increasing the hysteresis after +40V gate-voltage bias stress.

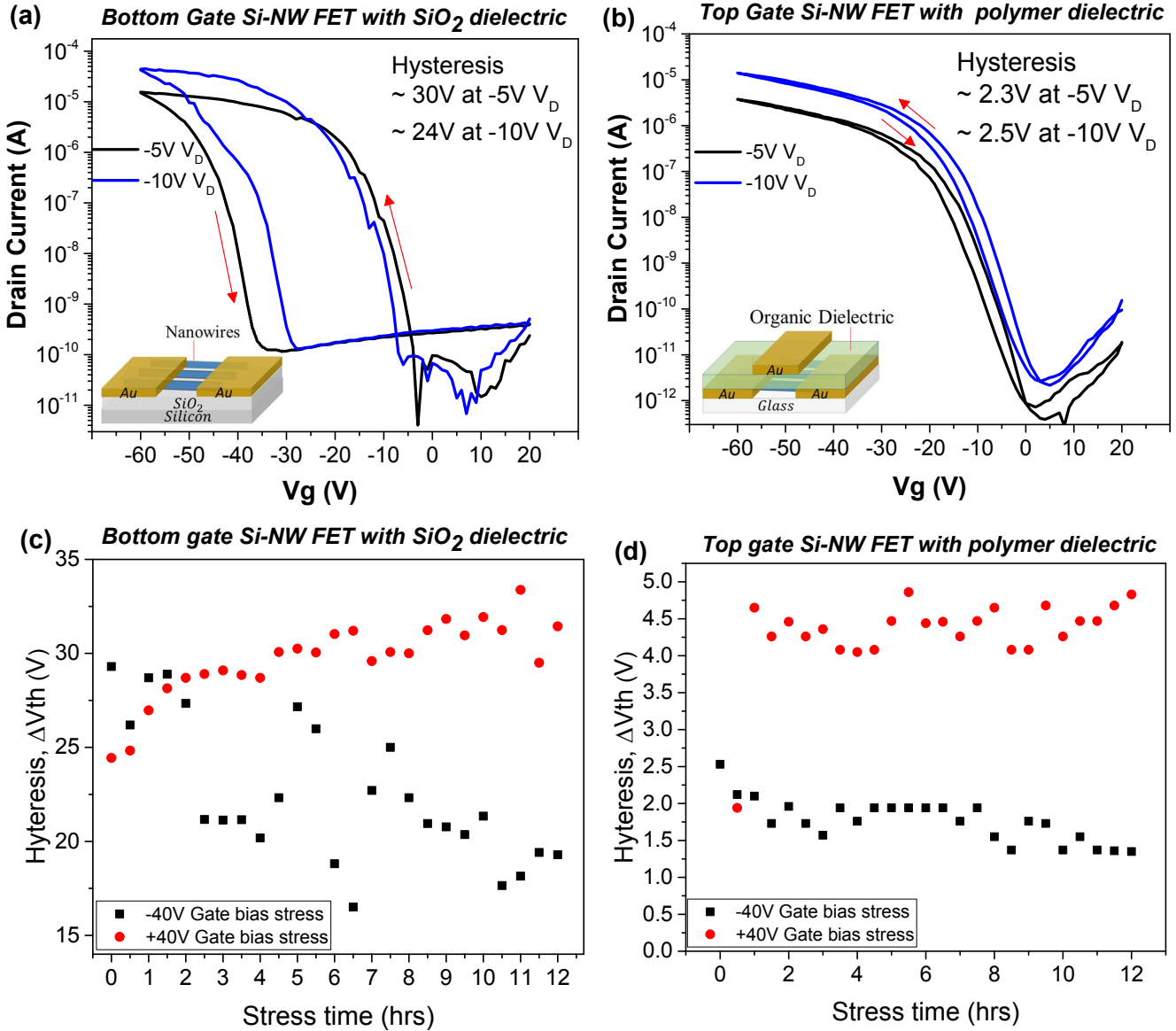


Figure 2. (a,b) transfer characteristics of Si NW FETs: (a) bottom gate FET with SiO₂ dielectric with 23 nanowires in the channel, showing a hysteresis value of ~30V at -5V drain voltage, with the inset showing the device architecture, (b) top gate FET with fluoropolymer dielectric with 4 nanowires in the channel, showing a hysteresis value of ~2.3V at -5V drain bias, with the inset showing the device architecture, (c) and (d) extracted hysteresis from the bias stress measurement for bottom gate SiO₂ dielectric FET and top gate devices with polymer dielectric, at -40V gate bias stress for 12hrs and +40V gate bias stress for 12hrs.

If we consider the hysteresis change and the shift of the threshold voltage after the bias stress in Si NW/SiO₂ FETs, these effects can be explained by the presence of both shallow and deep traps at the nanowire/SiO₂ interface. The shallow traps cause a change in hysteresis, whereas the deep traps, which take longer time to empty, causes the shift in the threshold voltage during the bias stress measurements[28]. Therefore, the shift in the threshold observed towards negative gate voltage during the -40V gate-voltage bias stress indicates the presence of deep hole traps at the Si NW/SiO₂ interface which screen the gate electric field. The positive shift in the threshold voltage during +40V gate bias indicates the de-trapping of holes, followed by possible electron trapping. However, the electron trapping is not significant as the threshold voltage shift is almost constant after the first stress period (30min). The absence of 'steps' or 'knees' in the subthreshold FET characteristics during the negative stress conditions indicates that no additional traps are formed (SI, Figure S4) [22, 29]. Therefore the main contributors of the strong hysteresis in Si NW FET using SiO₂ dielectric are the majority (holes) carrier traps at the Si NW/SiO₂ interface.

Figure 2(d) shows the extracted hysteresis from the transfer characteristics obtained after positive and negative gate-voltage bias stress for the top gate Si-NW/Cytop FET. The hysteresis decreased to $\sim 1.3\text{V}$ from an initial value of $\sim 2.5\text{V}$ after -40V gate voltage bias stress, and an increase in hysteresis to $\sim 4.8\text{V}$ was observed after $+40\text{V}$ gate voltage bias stress measurement. The observed change in hysteresis shows similar trend to Si-NW/SiO₂ FETs, indicating the filling and emptying of hole traps. The change in hysteresis is not that significant as compared to devices with SiO₂ dielectric, which suggests that lower density of traps is present at the Si-NW/Cytop interface. A shift in the threshold voltage to $\sim -22\text{V}$ was observed after -40V gate-voltage bias stress compared to an initial value of $\sim -13\text{V}$, whereas, a threshold voltage of $\sim -5\text{V}$ was achieved after $+40\text{V}$ gate-voltage bias stress (SI, Figure S5). The shift is constant after the first stress period for the positive bias indicating the absence of new electron traps introduced during the positive gate stress.

Overall, from the bias stress measurements conducted for Si nanowire FETs with SiO₂ and fluoropolymer dielectrics, we conclude that the majority of traps at the SFLS-grown Si-NW/dielectric interface are due to the shallow and deep hole traps, with significantly lower effect of trapping in the polymer top-gate dielectric devices, resulting in an order of magnitude reduction in hysteresis.

3.3 Double gate Si-NW FET

The direct one-to-one comparison of top gate and bottom gate devices presented in section 3.1 to study the NW/dielectric interface was not possible due to the differences in nanowire numbers present in the FET channels, and also due to possible variation in nanowires' properties including diameters, shell thicknesses, levels of impurities, and even Si core growth directions, resulting from non-uniform characteristics of as-synthesised SFLS nanowires[10, 30]. To be able to demonstrate the identical nanowire channel for bottom and top-gate transistor devices we have fabricated dual-gate FETs produced on the same substrate. The nanowires forming the FET channel were gated on the bottom by the SiO₂ dielectric, and on the top by the Cytop dielectric. These dual-gate structures allowed us to eliminate the variation of Si NW morphology, placement and the number of nanowires for the comparative studies of hysteresis effects in SiO₂ vs organic dielectric FETs. Figure 3 shows the transfer and output characteristics of a double-gate Si NW transistor with SiO₂ as bottom-gate dielectric and Cytop as top-gate dielectric, with 23 nanowires bridging the channel. Both the bottom gate and the top gate devices demonstrated excellent gate modulation, with an $I_{\text{ON}}/I_{\text{OFF}}$ ratio of $\sim 10^7$ for the bottom gate device and 3×10^6 for top gate Cytop device.

The hysteresis of the top gate organic dielectric device ($\sim 6\text{V}$) was much lower compared to the hysteresis of the bottom gate SiO₂ device ($\sim 31\text{V}$) (Fig.3a), due to lower trap density at the NW/organic dielectric interface, as we discuss below. These results are fully consistent with the measurements in section 3.1.

A higher I_{ON} at $V_{\text{D}} \sim -5\text{V}$ was observed for the bottom gate SiO₂ device compared to the top gate organic dielectric device, due to the higher dielectric value for the low thickness (230nm) of the SiO₂ insulator ($\epsilon_{\text{ins}}=3.9$) compared to the value of fluoropolymer dielectric ($\epsilon_{\text{ins}}=2.1$), for $1\mu\text{m}$ thick film. The extracted Si NW FET mobility of the top gate Cytop device of $12\text{ cm}^2/\text{Vs}$ is significantly higher than mobility of the bottom gate SiO₂ device of $1.7\text{ cm}^2/\text{Vs}$. The enhanced mobility for the top gate device can be attributed to the less scattering from trapped charge carriers in the Si NW/polymer dielectric interface.

The devices showed a near-Ohmic contact behavior, as observed in the output characteristics in Figure 3 (b,c). When both bottom and top gate were biased at the same time, there was an increase in I_{ON} and the hysteresis value ($\sim 22\text{V}$) was between the values obtained when biasing just the top and bottom gates individually (SI, Figure S6). The increase in I_{ON} can be due to the formation of the double channel around the nanowire at both the interfaces, resulting in more charge formation and better performance. When both the gates are biased, the double gate device acts as a gate all around FET to give a higher mobility and an enhanced performance [11, 31]. Charge accumulation at the same voltage is higher at Si NW/SiO₂ interface when compared to Si NW/Cytop interface, due to the higher capacitance of SiO₂ compared to Cytop.

We have evaluated the occupied trap density at the nanowire-dielectric interface related to the hysteresis using the following equation[18]:

$$NqQ_t = \frac{C_n \times |\Delta V_{th}|}{2 \pi r L_{NW}} \quad (3)$$

Where, q is the elementary charge and Q_t is the occupied trap density. Other notations are defined in Eq. 1-2. Typical radius (r) of Si nanowires is $\sim 20\text{nm}$ ($\pm 5\text{nm}$) and the nanowire length is estimated as the channel length ($5\mu\text{m}$) of the dual gate FET.

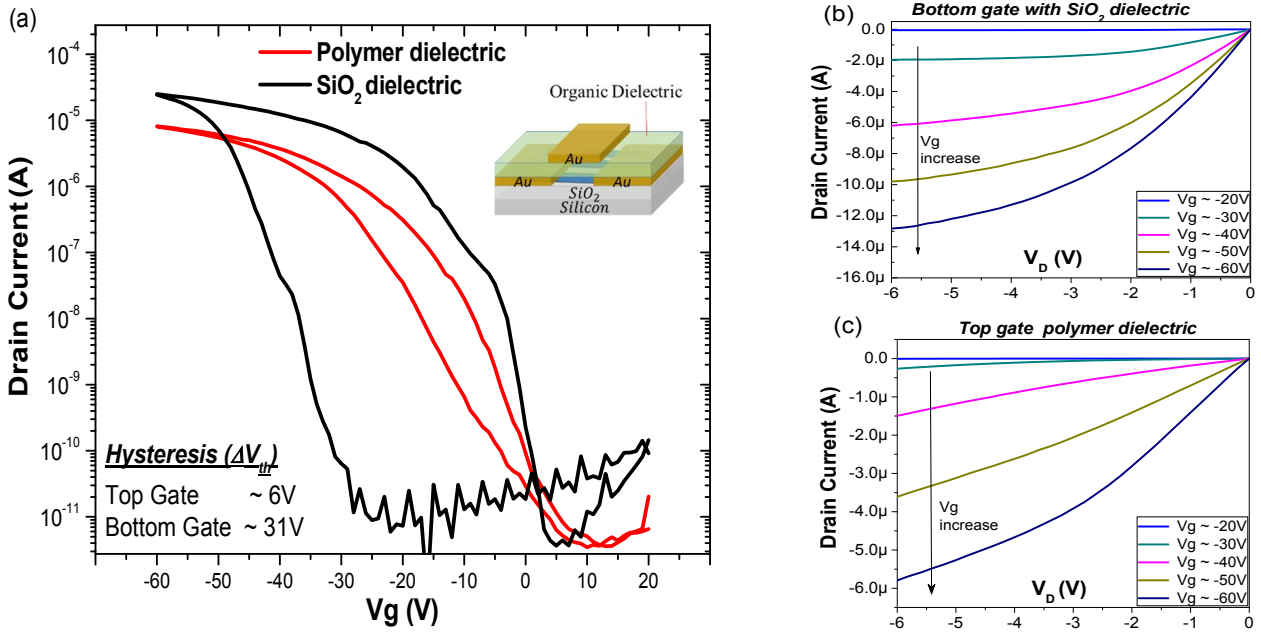


Figure 3. Transfer and output characteristics of the double gate Si NW FETs with SiO₂ bottom gate dielectric and fluoropolymer top gate dielectric: (a) transfer plots measurements of top gate and bottom gate devices (V_D -5V); (b-c) output characteristics of bottom gate and top gate FETs obtained by scanning drain voltage from 0 to -6V and measuring the drain current at constant gate voltages [-20V, -30V, -40V, -50V, -60V].

For the bottom gate SiO₂ operation FET, Q_t was evaluated to be $\sim 1 \times 10^{13} \text{ cm}^{-2}$ which is more than an order of magnitude higher compared to the Si NW/Cytop top gate operation FET $Q_t \sim 7.5 \times 10^{11} \text{ cm}^{-2}$. This difference shows that the Si NW/organic dielectric forms a higher quality lower-trapping interface compared to the Si NW/SiO₂ interface. Even lower trap density of $2.8 \times 10^{11} \text{ cm}^{-2}$ was evaluated for the top-gate FET device prepared on glass substrate with 2.3V hysteresis, demonstrated in section 3.1 (Fig. 2(b)).

Lower I_{OFF} of $3.6 \times 10^{-12} \text{ A}$ was observed for the forward scan of Si-NW/SiO₂ FET when compared to $1.5 \times 10^{-11} \text{ A}$ for reverse scan, demonstrating the effect of traps on the band bending at the NW interface. Higher band bending leads to higher Schottky barrier at the source/drain contacts, which will lower the I_{OFF} [18]. The subthreshold swing (SS) for the bottom gate FET was extracted to be 2V/decade, whereas the top gate device gave an SS of 4.3V/decade. The lower SS for bottom gate device is due to the higher dielectric constant of SiO₂ compared to the organic dielectric. It needs to be taken into account that the thickness of SiO₂ is ~ 4 times lower than the organic dielectric (1 μm). The increase in reverse SS compared to forward SS for bottom gate FET (from 2.7V/decade to 5.1V/decade) indicates the downward band bending inside the Si NW to the field near the SiO₂ interface, which depends on the trap density[18]. Top gate devices showed a small shift in SS for forward and reverse scans (5.6V/decade to 4.9V/decade) with negligible shift in I_{OFF} ($2 \times 10^{-12} \text{ A}$ to $1.6 \times 10^{-12} \text{ A}$) confirming the presence of less traps.

Finally, the standard (-40V) gate voltage bias stress was performed separately for the SiO₂ gate and the Cytop gate parts of the dual-gate FET. The hysteresis reduced from an initial value of $\sim 45 \text{ V}$ to $\sim 40 \text{ V}$ for SiO₂ dielectric after stress measurement, whereas Cytop dielectric gave $\sim 8 \text{ V}$ hysteresis following the stress measurements, compared to an initial value of $\sim 12 \text{ V}$ (SI, Figure S7). A shift in threshold voltage to negative values were also observed. The threshold voltage in SiO₂ dielectric FET shifted to $\sim -27.5 \text{ V}$ compared to an initial value of $\sim -21.4 \text{ V}$, however, Cytop dielectric showed a significant shift in threshold voltage from an initial value of $\sim -27 \text{ V}$ to $\sim -47 \text{ V}$ after the stress measurement. A reduced hysteresis and negative voltage shift in V_{th} observed for both the SiO₂ and Cytop devices, indicates the presence of shallow and deep hole traps at the interface.

4. Conclusions

Solution-processed silicon nanowires were deposited and aligned with low impurity content (NW clumps) on top of substrates using a roll-cast technique. Nanowire field-effect transistor devices in bottom- and top-gate

configurations with SiO₂ and Cytop polymer gate dielectrics were fabricated. Electrical analysis of the FETs demonstrated dramatic reduction of hysteresis from up to 40V in SiO₂ gated devices to only 2.3V in Cytop-gated transistor. Both individual bottom gate (SiO₂) and top-gate (Cytop) FETs, as well as dual-gate devices show the same trend of very low hysteresis for the hydrophobic polymer gate dielectric. The change in hysteresis behavior is linked with over 10 times lower occupied trap density at the nanowire-fluoropolymer dielectric interface of $2.3 \times 10^{11} \text{ cm}^{-2}$ (Cytop) vs $1 \times 10^{13} \text{ cm}^{-2}$ (SiO₂). Gate bias stress studies confirmed that the trapping of holes is taking place, as shown by the lower hysteresis ($\sim 19.3\text{V}$) after 12hr negative (-40V) gate voltage stress, but an elevated hysteresis ($\sim 31.4\text{V}$) after +40V bias, also indicating the presence of fast filling shallow traps at the nanowire-dielectric interface. The shift in threshold after the prolonged positive and negative gate bias voltages indicated the presence of deep, slow filling hole traps which screen the gate electric field. Finally, higher Si NW FET mobility of $12 \text{ cm}^2/\text{Vs}$ observed for Cytop dielectric device compared to $1.7 \text{ cm}^2/\text{Vs}$ for Si-NW/SiO₂ FET confirms the lower degree of charge carrier scattering at the nanowire/polymer interface, fully consistent with the lower trap density.

The demonstrated silicon nanowire transistors with solvent based processing of both semiconducting channel and dielectric layer open up possibilities for low-cost printing technologies for nanomaterials- based electronic devices.

Acknowledgements

MS would like to acknowledge support from EPSRC UK grant EP/I017569/1.

References

1. Nair R S, Perret E, Tedjini S and Baron T 2013 A group-delay-based chipless RFID humidity tag sensor using silicon nanowires *IEEE Antennas and Wireless Propagation Letters* **12** 729-732
2. Lloyd J S, Fung C M, Deganello D, Wang R J, Maffei T G G, Lau S P and Teng K S 2013 Flexographic printing-assisted fabrication of ZnO nanowire devices *Nanotechnology* **24** 195602-195602
3. Seo K, Lim T, Kim S, Park H-L and Ju S 2010 Tunable-white-light-emitting nanowire sources *Nanotechnology* **21** 255201-255201
4. Ong Y Y, Chen B T, Tay F E H and Iliescu C 2006 Process Analysis and Optimization on PECVD Amorphous Silicon on Glass Substrate *Journal of Physics: Conference Series* **34** 812-817
5. Zschieschang U, Ante F, Yamamoto T, Takimiya K, Kuwabara H, Ikeda M, Sekitani T, Someya T, Kern K and Klauk H 2010 Flexible low-voltage organic transistors and circuits based on a high-mobility organic semiconductor with good air stability *Advanced Materials* **22** 982-985
6. Cui Y, Zhong Z H, Wang D L, Wang W U and Lieber C M 2003 High performance silicon nanowire field effect transistors *Nano Letters* **3** 149-152
7. Huang Y, Duan X, Wei Q and Lieber C M 2001 Directed assembly of one-dimensional nanostructures into functional networks *Science* **291** 630-633
8. Suzuki H, Araki H, Tosa M and Noda T 2007 Formation of Silicon Nanowires by CVD Using Gold Catalysts at Low Temperatures *Materials Transactions* **48** 2202-2206
9. Surawijaya A, Anshori I, Rohiman A and Idris I 2011 Silicon nanowire (SiNW) growth using Vapor Liquid Solid method with gold nanoparticle catalyst *Proceedings of the International Conference on Electrical Engineering and Informatics* 19-21
10. Hanrath T and Korgel B a 2003 Supercritical fluid-liquid-solid (SFLS) synthesis of Si and Ge nanowires seeded by colloidal metal nanocrystals *Advanced Materials* **15** 437-440

11. Wang M C P and Gates B D 2009 Directed assembly of nanowires *Materials Today* **12** 34-43
12. Kang J, Myung S, Kim B, Oh D, Kim G T and Hong S 2008 Massive assembly of ZnO nanowire-based integrated devices *Nanotechnology* **19** 095303-095303
13. Acharya S, Panda A B, Belman N, Efrima S and Golan Y 2006 A semiconductor-nanowire assembly of ultrahigh junction density by the Langmuir-Blodgett technique *Advanced Materials* **18** 210-213
14. Li X, Zhang L, Wang X, Shimoyama I, Sun X, Seo W K and Dai H 2007 Langmuir-Blodgett assembly of densely aligned single-walled carbon nanotubes from bulk materials *Journal of the American Chemical Society* **129** 4890-4891
15. Raychaudhuri S, Dayeh S A, Wang D and Yu E T 2009 Precise semiconductor nanowire placement through dielectrophoresis *Nano Letters* **9** 2260-2266
16. Freer E M, Grachev O, Duan X, Martin S and Stumbo D P 2010 High-yield self-limiting single-nanowire assembly with dielectrophoresis *Nature nanotechnology* **5** 525-530
17. Kim D K, Lai Y, Vemulkar T R and Kagan C R 2011 Flexible, low-voltage, and low-hysteresis PbSe nanowire field-effect transistors *ACS Nano* **5** 10074-10083
18. Paska Y 2012 Interactive Effect of Hysteresis and Surface Chemistry on Gated Silicon Nanowire Gas Sensors *ACS Applied Materials & Interfaces* **4** 2604-2617
19. Cassé M, Thevenod L, Guillaumot B, Tosti L, Martin F, Mitard J, Weber O, Andrieu F, Ernst T, Reibold G, Billon T, Mouis M and Boulanger F 2006 Carrier Transport in HfO₂ / Metal Gate MOSFETs : Physical Insight Into Critical Parameters **53** 759-768
20. Wang Y W Y, Lew K-K L K-K, Mattzela J, Redwing J and Mayer T 2005 Top-gated field effect devices using oxidized silicon nanowires *63rd Device Research Conference Digest, 2005. DRC '05.* **1** 2004-2005
21. Kawashima T, Saitoh T, Komori K and Fujii M 2009 Synthesis of Si nanowires with a thermally oxidized shell and effects of the shell on transistor characteristics *Thin Solid Films* **517** 4520-4526
22. Lustig N and Kanicki J 1989 Gate dielectric and contact effects in hydrogenated amorphous silicon-silicon nitride thin-film transistors *Journal of Applied Physics* **65** 3951-3957
23. Spijkman M J, Myny K, Smits E C P, Heremans P, Blom P W M and De Leeuw D M 2011 Dual-gate thin-film transistors, integrated circuits and sensors *Advanced Materials* **23** 3231-3242
24. Opoku C, Chen L, Meyer F and Shkunov M. *Solution processable nanowire field-effect transistors.* in *MRS Proceedings*. 2011. Cambridge Univ Press, mrsf10-1287-f10-03
25. Duan X, Niu C, Sahi V, Chen J, Parce J W, Empedocles S and Goldman J L 2003 High-performance thin-film transistors using semiconductor nanowires and nanoribbons *Nature* **425** 274-278
26. Goldberger J, Sirbuly D J, Law M and Yang P 2005 ZnO nanowire transistors *The journal of physical chemistry. B* **109** 9-14
27. Opoku C, Hoettges K F, Hughes M P, Stolojan V, Silva S R P and Shkunov M 2013 Solution processable multi-channel ZnO nanowire field-effect transistors with organic gate dielectric *Nanotechnology* **24** 405203-405203
28. Egginger M, Bauer S, Schwödiauer R, Neugebauer H and Sariciftci N 2009 Current versus gate voltage hysteresis in organic field effect transistors *Monatshefte für Chemie - Chemical Monthly* **140** 735-750
29. Georgakopoulos S, Sparrowe D, Meyer F and Shkunov M 2010 Stability of top- and bottom-gate amorphous polymer field-effect transistors *Applied Physics Letters* **97** 243507
30. Holmes J D 2000 Control of Thickness and Orientation of Solution-Grown Silicon Nanowires *Science* **287** 1471-1473

31. Yeo K H, Suk S D, Li M, Yeoh Y-y, Cho K H, Hong K-H, Yun S, Lee M S, Cho N and Lee K. Gate-all-around (GAA) twin silicon nanowire MOSFET (TSNWFET) with 15 nm length gate and 4 nm radius nanowires, *2006 International Electron Devices Meeting*, 1-4

Supporting Information

Electrical analysis of hysteresis in solution processed silicon nanowire field effect transistors

K. Prabha Rajeev, C. Opoku, V. Stolojan, M. Constantinou and M. Shkunov*

Electronic Engineering, Advanced Technology Institute, University of Surrey, Guildford GU2 7XH, UK

* email: m.shkunov@surrey.ac.uk

Deposition and alignment of silicon nanowires

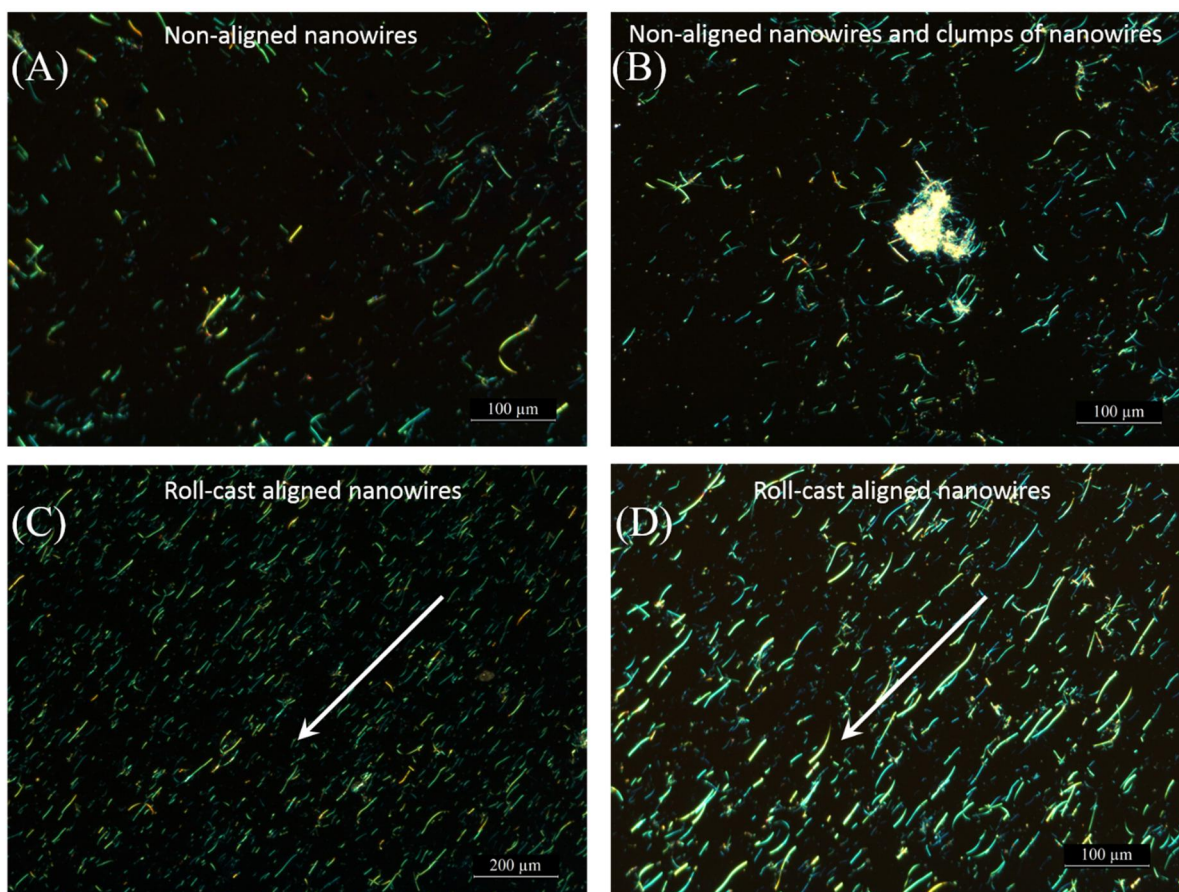


Figure S1. Polarised optical microscope images of SFLS grown silicon nanowire on Si/SiO₂ substrates: (A) non-aligned nanowires deposited by drop-casting, (B) non-aligned nanowires, with clumps of nanowires on the substrate after drop-casting deposition, (C) and (D) roll-cast aligned nanowires with no clumps of nanowires/particles, arrow represents the direction of alignment.

Hysteresis and I_{ON}/I_{OFF} calculations

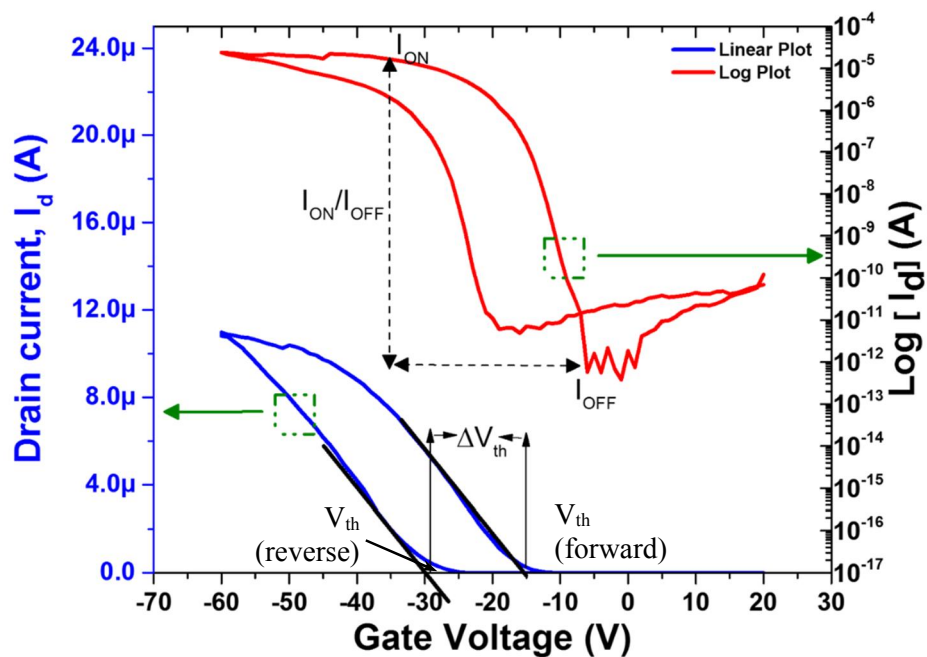


Figure S2. Linear regime transfer characteristic of a typical Si-NW FET in a linear and a log-linear scale. Forward V_g scan is from +20V to -60V, immediately followed by a reverse V_g scan from -60V to +20V. Hysteresis ΔV_{th} is extracted from the linear plot by taking the difference between the threshold voltages for the forward and for the reverse scans. Threshold voltage is defined as the intersect of a linear fit to the I-V curves and the zero-current axis. I_{ON}/I_{OFF} current ratio is extracted from the log plot, by taking the ratio of maximum current obtained during accumulation and the current when the FET is in the ‘off’ state.

Hysteresis measurements for bottom gate SiO₂ dielectric FETs and top gate polymer dielectric FETs.

Data for nine devices of each type is shown. The hysteresis values for SiO₂ dielectric FETs are in the 15V to 40V range. Devices with Cytop dielectric demonstrate significantly lower hysteresis between 2V and 10 V, with 50% of devices showing ΔV_{th} of less than 3V.

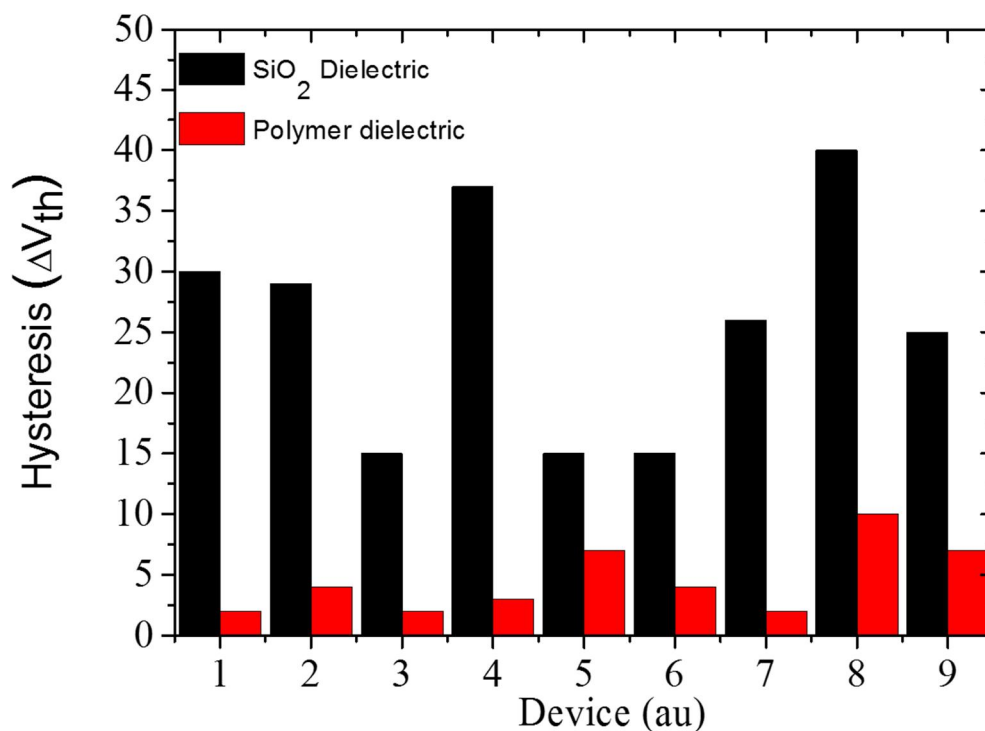


Figure S3. The histogram showing the difference in observed hysteresis for various bottom gate Si NW FET with SiO₂ dielectric and top gate fluoropolymer Si NW FET. Hysteresis was extracted from transfer I-V measurements conducted at $V_D \sim -6V$.

Bias stress measurements

Si nanowire FETs with bottom gate SiO₂ dielectric

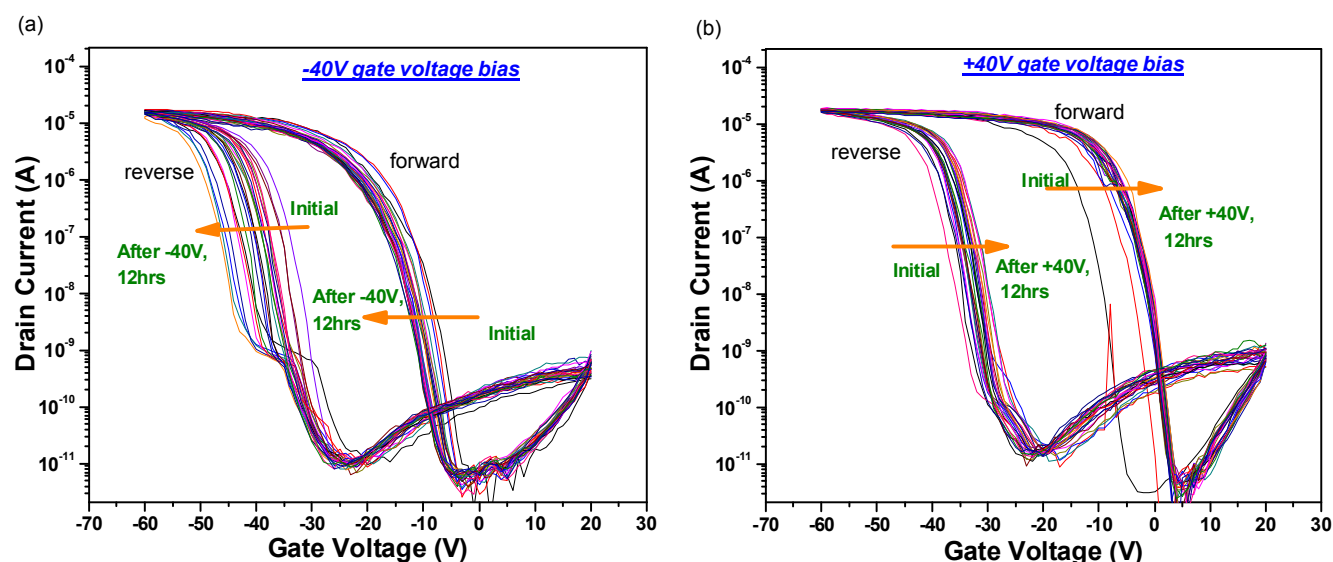


Figure S4. Transfer characteristics of bottom gate Si NW FETs with SiO₂ dielectric.

(a) transfer characteristics extracted during the gate voltage bias stress measurements with -40 V gate voltage stress, when $V_g = -40V$ applied for 30min & I-Vs measured immediately after, followed by the next cycle of bias stress. Repeated cycles of stress/measurements continued for a total for 12hrs of stress time.

(b) transfer characteristics extracted during the gate voltage bias stress measurements with +40V gate voltage stress, when $V_g = +40V$ applied for 30min & I-Vs measured immediately after, followed by the next cycle of bias stress. Repeated cycles of stress/measurements continued for a total for 12hrs of stress time.

We note that a shift in threshold voltage towards more negative values is observed after negative gate-bias stress, whereas the threshold voltage shifted to positive voltages after positive gate-bias stress.

Bias stress measurements

Si nanowire FETs in top gate configuration with Cytop dielectric

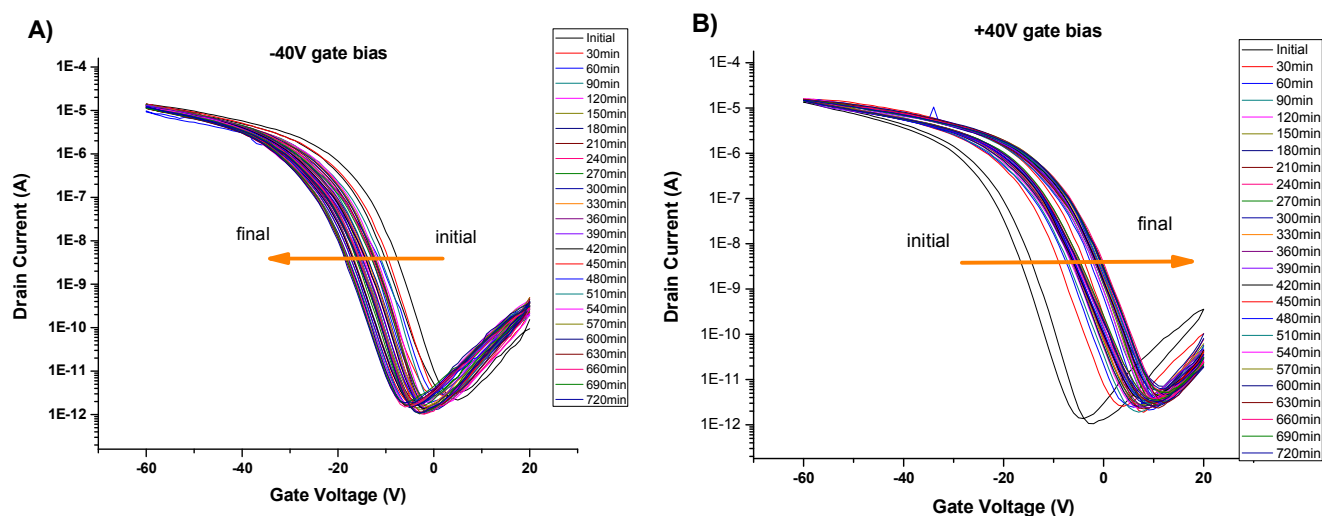


Figure S5. Gate voltage bias stress measurements of top gate device with fluoropolymer Cytop dielectric. I-Vs measured at $V_D = -10V$.

(a) Gate bias voltage stress at -40V with a hold time of 30min followed by measurements, cycles repeated for 12hrs. A shift in threshold to more negative voltages is observed.

(b) Gate bias voltage stress at +40V with a hold time of 30min followed by measurement, cycles repeated for 12hrs. Data shows a shift in threshold to the positive gate voltages after the first stress time, but the positive threshold voltage shift is smaller for the next measurements.

Dual gate Si nanowire devices

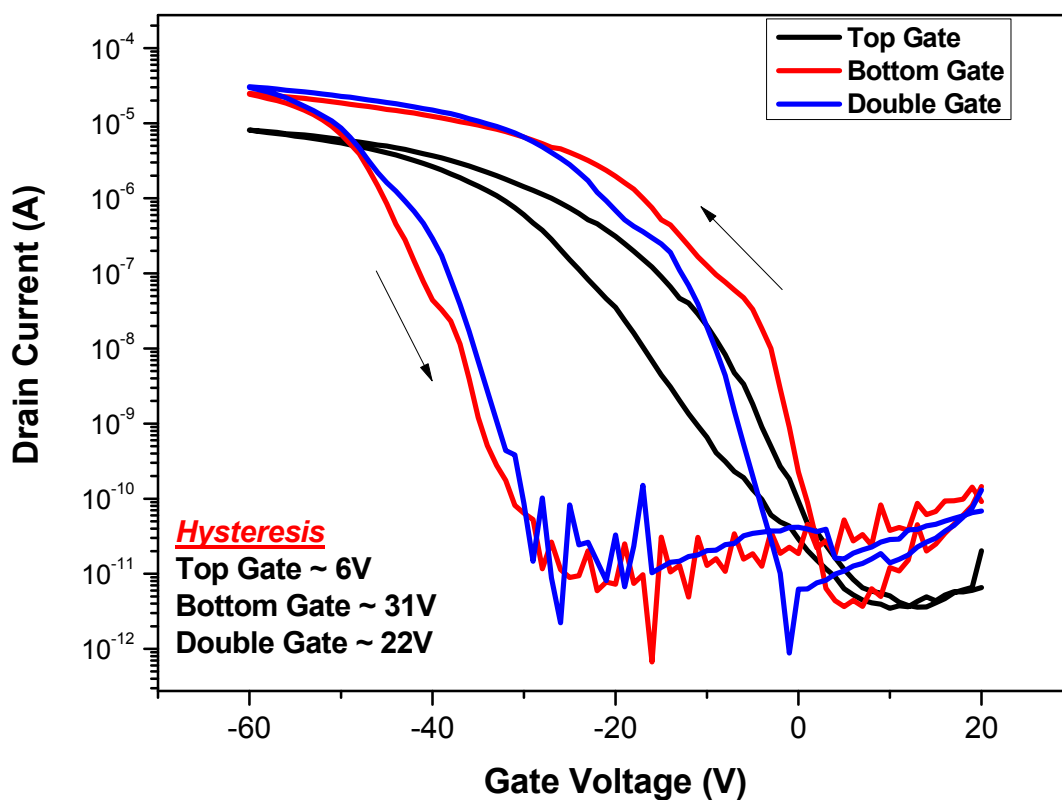


Figure S6. Transfer characteristics of the double gated Si nanowire transistor showing individual gate bias characteristics as well as the double gate bias characteristics: red curve – only bottom gate SiO₂ is biased, black curve- only top polymer gate is biased, blue curve – both top and bottom gates are biased simultaneously. Results: ~ 6V hysteresis for Si NW/organic dielectric interface and ~ 31V hysteresis for Si NW/SiO₂ interface. When both the gates are biased together, hysteresis reduced to ~ 22V when compared to Si NW/SiO₂ interface, and a higher ON current is also observed, compared to top-gate operation.

Dual gate Si NW FET bias stress measurements: each interface (nanowire SiO₂) and nanowire/polymer were measured separately.

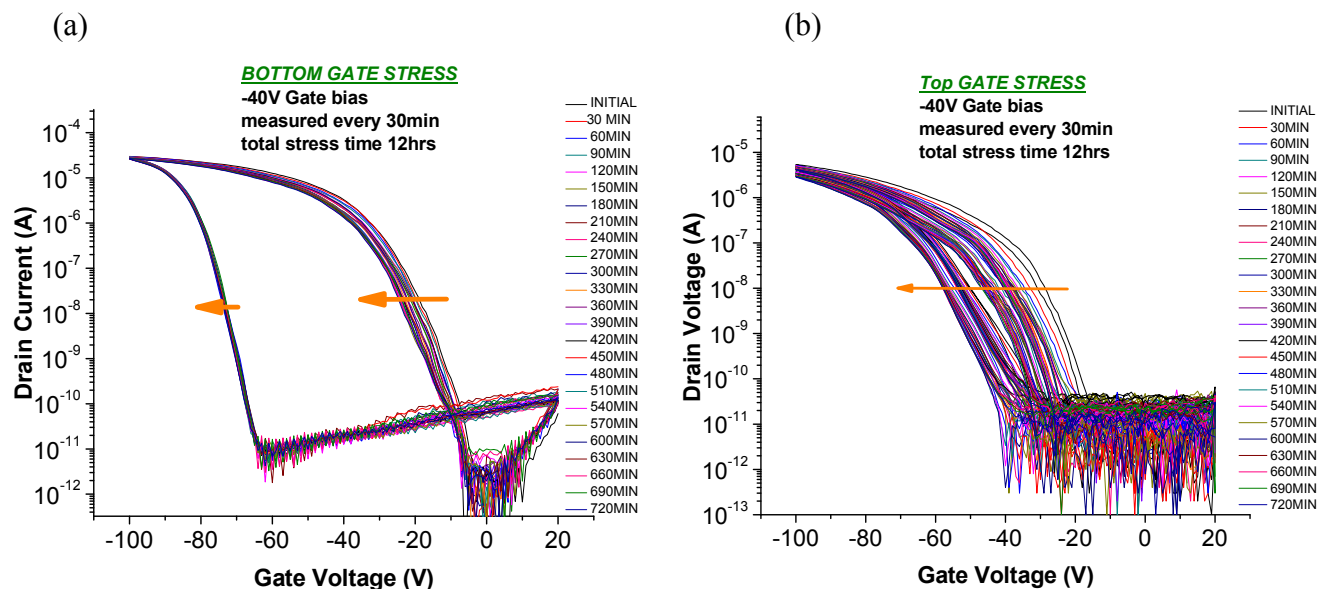


Figure S7. Bias stress measurements of dual gate Si NW FET with bottom SiO₂ dielectric and top gate fluoropolymer dielectric. (a) Bottom gate device bias voltage stress at -40V with a hold time of 30min followed by measurement, cycles repeated for 12hrs. Data shows a shift in threshold to the negative gate voltages. (b) Top gate device bias voltage stress at -40V with a hold time of 30min followed by measurement, cycles repeated for 12hrs. Results demonstrate a shift in threshold to more negative gate voltages.